

On the DC Inductors Size Reduction in a Multi-Cell Topology based on Current Source Converters by Means of Magnetic Couplings

Pedro E. Melin ♠ Carlos R. Baier ♣ José R. Espinoza ♦ Javier A. Muñoz ♣ Roberto R. Ramirez ♦ Eduardo A. Maurelia ♦

♠ Department of Electrical and Electronic Engineering, Universidad del Bío-Bío, Concepción, CHILE,

♦ Department of Electrical Engineering, Universidad de Concepción, Concepción, CHILE,

♣ Department of Industrial Technologies, Universidad de Talca, Curicó, CHILE,
pemelin@ubiobio.cl cbaier@utalca.cl Jose.Espinoza@udec.cl

Abstract— This work deals with a multi-cell topology based on current-source converters based power cells. The main disadvantage of this configuration is the bulky DC inductor required in each cell which must be designed in order to compensate the oscillating power drained by the single-phase inverter. In order to avoid the use of a large DC inductor, the use of magnetic couplings among DC links of different power cells is considered. Additionally, active front end rectifiers are used in order to control the DC current and ensure a unitary displacement power factor in each power cell. A control scheme based on non-linear controllers is proposed in order to control each cell in a decoupled way. The topology feasibility is tested experimentally, while the control scheme performance is tested by simulation, showing that it is possible to obtain an excellent overall input current quality and a load voltage with lesser dv/dt than the classic multi-cell topology, reducing the required DC inductor from 400 mH to 30 mH for the studied case.

Keywords—Current-Source Converters, Cascaded H-Bridge based on Current-Source Inverters, Non-linear Control

I. INTRODUCTION

Multicell topologies are widely used in medium-voltage AC drives mainly due to the possibility of using semiconductors with standard voltage ratings. The cascaded H-Bridge multilevel topology consists in single-phase inverters connected in a series array in order to obtain a higher load voltage. Each inverter is fed by a rectifier stage through a DC link. The main advantage of multicell topologies are (i) the use of devices with lower voltage rating than the output voltage of the converter, (ii) reliability due to the use of a modular topology that allows to replace a damaged inverter while the others are still operating, (iii) lower dv/dt than NPC or CFB topologies when more than three cells per phase are used and (iv) low distortion of the input current due to the use of a multi-step transformer that allows to compensate harmonic currents by the magnetic flux cancellation in the core [1],[2]. While its main disadvantages are (i) topology complexity and (ii) complex and bulky multi-pulse transformer, which must be constructed to achieve secondary phase-shifted voltages in order to compensate the harmonic currents, especially when a diode bridge or a phase-controlled rectifier is used.

On the other hand, current-source inverters (CSI) are also widely used in power drives [3],[4]. Their main advantage are the low distortion in the load voltage, the inherent protection against short circuits and a similar efficiency with respect to VSC topologies if the load voltage control is done by the DC current [5]. In order to get a multilevel topology, n CSIs can be connected to the load in a parallel array using a common capacitive filter and modulated in an appropriate way in order to add up their currents and to compensate some harmonics, obtaining a resulting current with $2n + 1$ levels[9]-[14]. This kind of topologies allows dividing the load current in n inverters, but each inverter must be designed to hold the total load voltage. Thus, requiring the use of several semiconductors in a series array to form a switch in order to increase the blocking voltage and the use of a capacitive filter with a voltage rating higher than the load voltage. Another option is to connect n inverters in a cascaded array – each one with a capacitive filter –, allowing to use devices with standard voltage rating to feed a load with a higher voltage. In this case, it is necessary the use of single-phase inverters, without the possibility to obtain a multilevel current. However, the output AC capacitor allows to compensate voltage harmonics and to obtain a load voltage with less distortion than each output by itself [16]-[20]. On the other hand, the oscillating power in the DC link of a power cell drained by each inverter can lead to an unwanted oscillation in the DC current, which is considered a perturbation.

This work deals with a multi-cell topology based on current source converters in order to reduce the DC inductor size. The design of the DC inductor for a non-compensated oscillating power is revised and the use of magnetic couplings in the DC links to compensate the oscillating power is analyzed. Additionally, an appropriate control scheme for an active front end cell is proposed, which allows to control the cell output voltage through the DC current and to ensure a desired displacement power factor in the cell input current. Preliminary experimental results show the feasibility of the oscillating power compensation, while simulated results complement the performance of the proposed control scheme.

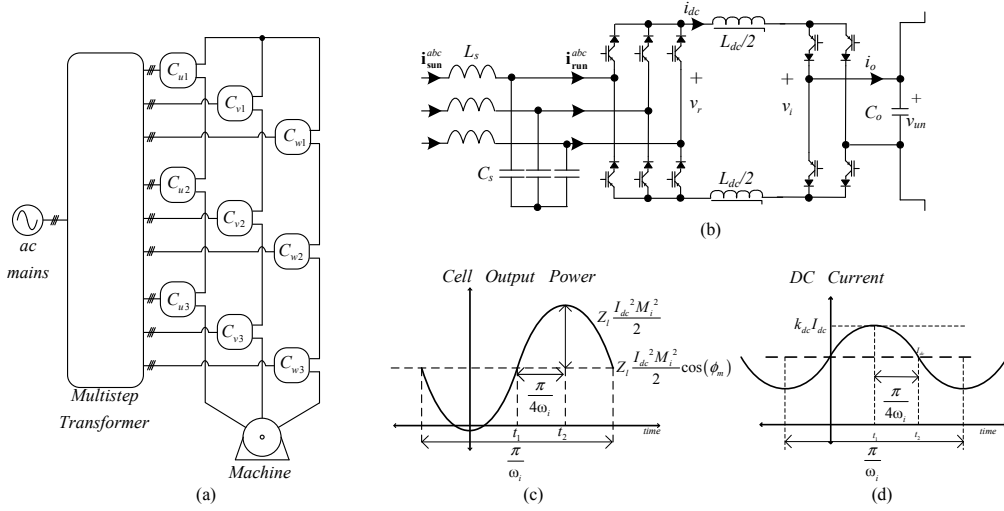


Fig. 1 Multi-cell topology based on current source converter; (a) multi-cell topology; (b) three-phase/single-phase current source cell; (c) power drained by the inverter to the DC link; (d) DC current variation by the oscillating power.

II. MULTI-CELL CURRENT SOURCE TOPOLOGY

A. Description of the Multi-Cell Topology

The proposed topology is build up by $3n_C$ current-source based cells where n_C cells are connected in a cascaded array in order to feed a common phase (Fig. 1a). A capacitive filter is required in the AC side of each inverter which provides a low impedance path for current harmonics, decreasing the di/dt in the load and providing – in combination with the inverter – a controlled voltage source which can be connected in a series array with other inverters. At the input of the topology a transformer with $3n_C$ secondary windings are used to step-down the cell input voltage – allowing the use of semiconductors with low voltage rating – and reducing the input current distortion by the magnetic flux cancellation in the core. The transformer can be a multi-pulse transformer as used in VSC based multicell topologies and can be simplified if an active front end rectifier is used. The inverters are fed from a controlled rectifier through an inductive DC link that behaves as a controlled current source (Fig. 1b). In the AC side of each rectifier, a second-order LC filter is required. This filter can be implemented using some or all the leakage inductance of the transformer secondary. It has a resonance in $1/(2\pi\sqrt{LC})$ Hz that should be considered when the filter is designed [6]. For this work an active front end rectifier is used, which allows to regulate the DC link current and to control the input displacement power factor of the power cell.

Each cell can be mathematically modeled considering Fig. 1 and the work presented in [7]. The resulting equations are:

$$\mathbf{v}_s^{abc} = L_s \frac{d}{dt} \mathbf{i}_s^{abc} + \mathbf{v}_{C_s}^{abc}, \quad (1)$$

$$\mathbf{i}_s^{abc} = C_s \frac{d}{dt} \mathbf{v}_{C_s}^{abc} + \mathbf{s}_r^{abc} i_{dc}, \quad (2)$$

$$\left[\mathbf{s}_r^{abc} \right]^T \mathbf{v}_{C_s}^{abc} = L_{dc} \frac{d}{dt} i_{dc} + s_i i_{dc}, \quad (3)$$

$$v_o = R_l i_o + L_s \frac{d}{dt} i_o. \quad (4)$$

The system presented in (1) – (4) is non-linear and coupled. The equation that models the DC side is,

$$s_i i_{dc} = C_o \frac{d}{dt} v_o + i_l, \quad (5)$$

where s_i is the inverter switching function and i_l is the load current. In order to get an average model for (1) - (5) the switching function can be reduced to its fundamental component. Thus,

$$s_i \approx m_i = G_i M_i \sin(\omega_l t + \alpha_i), \quad (6)$$

$$\mathbf{s}_r^{abc} \approx G_r \mathbf{m}_r^{abc}. \quad (7)$$

Using these equations, the oscillating power drained by the single-phase inverter from the DC link can be characterized and a DC inductor can be designed in order to compensate it.

B. Oscillating Power and DC Inductor

The oscillating power drained from the DC link to the inverter is given by

$$p_o = S_o \left[\cos(\phi_m) - \cos(2\omega_l t + 2\alpha_i + \phi_m) \right], \quad (8)$$

where S_o is the inverter apparent power that can be defined by

$$S_o = Z_m I_{dc}^2 M_i^2 / 2, \quad (9)$$

and where Z_m is the equivalent impedance of the load and the capacitor filter connected in parallel. The instantaneous power waveform drained by the inverter is shown in Fig. 1c, where there is a continuous component which is the load active power, and an oscillating power whose amplitude is equal to S_o and frequency equal to twice the inverter frequency. The continuous component is injected to the DC link by the rectifier which is controlled in order to keep the DC current level, while the DC inductor provides the oscillating component. The oscillating power causes an oscillating DC current (Fig. 1d) that can be obtained from

$$\frac{L_{dc} \left[i_{dc}(t_2)^2 - i_{dc}(t_1)^2 \right]}{2(t_2 - t_1)} = p_o(t_2) - p_o(t_1). \quad (10)$$

Considering $i_{dc}(t_1) = I_{dc}$ and $i_{dc}(t_2) = I_{dc} k_{dc}$, where if k_{dc} is close to 1 there is no variation of the DC current i_{dc} , then,

$$4\omega_i \pi^{-1} L_{dc} I_{dc}^2 \left[(k_{dc})^2 - 1 \right] = S_o, \quad (11)$$

and if (9) is included in order to solve for k_{dc} it is found that,

$$k_{dc} = \sqrt{\frac{\pi Z_m M_i^2}{8\omega_i L_{dc}} + 1}. \quad (12)$$

This equation shows that the DC current variation decreases when the inverter frequency or DC inductor increases. The DC current variation due to the oscillating power causes unwanted frequency components in the load voltage side and in the input current of the power cell. This can produce resonances in the LC input filter or the LC equivalent circuit given by the output capacitor and the inductive load. A large DC inductor can be selected in order to get a k_{dc} close to the unity, but it involves an increasing cost, size and I^2R losses.

C. CSC Cells with DC Links Magnetically Coupled

In order to compensate the oscillating power, three CSC cells feeding different load phases and with their DC links magnetically coupled are studied (Fig. 2). Considering the above, it is possible to mitigate even harmonics with positive or negative sequences excited by inverters whose output voltages are 120° phase-shifted. Zero sequence currents (6^{th} and multiples provided by the load) must be mitigated by the DC inductor [18].

Neglecting the switching harmonic frequencies, an average model can be used in order to analyze the DC links of the magnetically coupled cells. Then, the rectifier DC voltage in an arbitrary x -th cell, v_{rx} , can be expressed as

$$v_{rx} = G_r \mathbf{m}_{rx}^{abc} \left[\mathbf{v}_{C_{fx}}^{abc} \right]^T, \quad (13)$$

and the inverter DC voltage is defined by

$$v_{ix} = \frac{M_x V_i}{2} \left[\cos(\phi_i) - \cos(2\theta_i + 2\alpha_x + \phi_i) \right]. \quad (14)$$

On the other hand, if the magnetizing inductance and resistance are considered high enough, both can be neglected. Therefore, the harmonic voltages at the primary and secondary of each magnetic coupling are equal. If the magnetic coupling between the DC links have identical parameters, thus

$$L_{uw} = L_{vu} = L_{vw} = L, \quad (15)$$

where L_{xy} is the mutual inductance as shown in Fig. 2. It is known that the mutual inductance for a magnetic coupling between two identical windings is

$$M = k\sqrt{L^2}, \quad (16)$$

where, if the coupling factor $k = 1$ then L is equal to M for each DC link ($M = L$). Hence, the coupling voltages shown in Fig.2, can be written as,

$$\begin{bmatrix} v_M^{uv} \\ v_M^{vw} \\ v_M^{wu} \end{bmatrix} = - \begin{bmatrix} v_M^{wu} \\ v_M^{vw} \\ v_M^{uv} \end{bmatrix} = M \begin{bmatrix} 1 & -1 & 0 \\ 0 & 1 & -1 \\ -1 & 0 & 1 \end{bmatrix} \begin{bmatrix} \frac{d}{dt} i_{dcu} \\ \frac{d}{dt} i_{dcv} \\ \frac{d}{dt} i_{dcw} \end{bmatrix}. \quad (17)$$

From (17) and using KVL for each DC link shown in Fig.2, it is possible to write

$$v_{ru} = v_{zu} - v_M^{wu} + v_{iu} + v_M^{uv}, \quad (18)$$

$$v_{rv} = v_{zv} - v_M^{uv} + v_{iv} + v_M^{vw}, \quad (19)$$

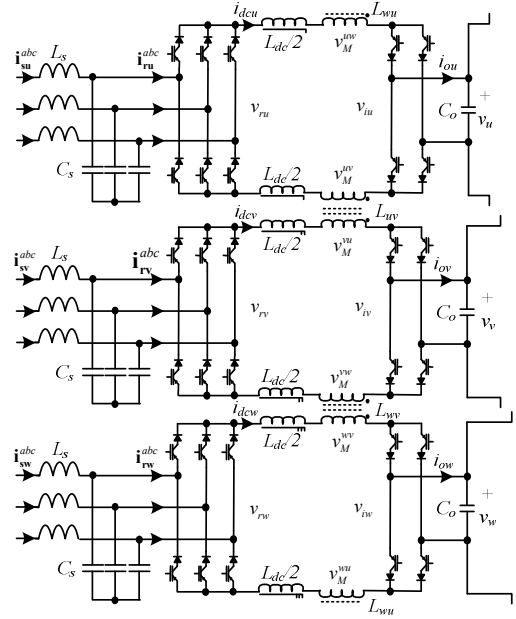


Fig. 2 Multi-cell topology with magnetic coupling.

$$v_{rw} = v_{zw} - v_M^{vw} + v_{iw} + v_M^{wu}, \quad (20)$$

where v_{zx} is the voltage in Z_x which includes the DC inductor components (inductance L_{dcx} and resistance R_{dcx}) and the transformer leakage impedance. If the DC link impedances are identical, then

$$v_z = v_{zu} = v_{zv} = v_{zw}. \quad (21)$$

From the previous equations, it is possible to determine that the Z_x voltage in each coupled cell satisfies

$$v_z = \frac{1}{3} \left[(v_{ru} + v_{rv} + v_{rw}) - (v_{iu} + v_{iv} + v_{iw}) \right], \quad (22)$$

where using (14), each coupled cell inverter voltage can be written as

$$v_{iu} = \frac{M_u V_u}{2} \left(1 - \cos(2\theta_i + \phi_i) \right), \quad (23)$$

$$v_{iv} = \frac{M_v V_v}{2} \left(1 - \cos\left(2\theta_i + \frac{2}{3}\pi\right) \right), \quad (24)$$

$$v_{iw} = \frac{M_w V_w}{2} \left(1 - \cos\left(2\theta_i + \frac{4}{3}\pi\right) \right), \quad (25)$$

and replacing (23), (24) and (25) in (22) as

$$v_z = \frac{1}{3} \left[(v_{ru} + v_{rv} + v_{rw}) - \frac{1}{2} (M_u V_u + M_v V_v + M_w V_w) \right], \quad (26)$$

where the oscillating term in the inverters voltages are compensated because they are 120° out of phase.

III. PROPOSED CONTROL SCHEME

The control objectives are (i) load voltage regulation and (ii) input displacement power factor. The load voltage can be regulated through the regulation of each power cell output voltage while the displacement power factor can be controlled at the input of each power cell. Then, the cell output frequency and phase are imposed by the inverter by means of the modulating technique, while the output voltage amplitude is

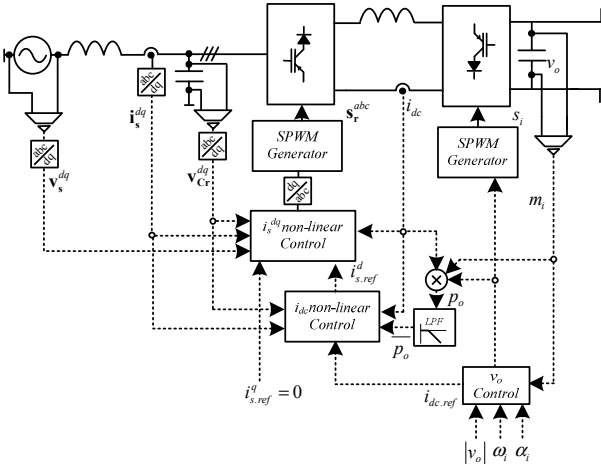


Fig. 3 Control scheme for each cell

set by the DC current level, which is regulated by the rectifier stage that also controls the input displacement power factor.

The proposed control scheme is focused in the decoupled control of each cell using input/output linearization as described in [8], where both the DC current and the displacement power factor are controlled. A master control is used to set the references in order to impose the load voltage through the DC current and the displacement power factor controlled by the power cell input current, Fig. 3. The use of non-linear control is justified because the cells are non-linear and coupled systems as shown in Section II, and because there is a high dependence between the operating point and the DC current level that must be set in order to control the cell output voltage.

A state model in the dq frame is needed in order to define the control expressions. Then, using the Park transformation for (1)-(5), it is obtained,

$$\mathbf{v}_s^{dq} = L_s \frac{d}{dt} \mathbf{i}_s^{dq} + L_s \mathbf{W} \mathbf{i}_s^{dq} + \mathbf{v}_{Cr}^{dq} \quad (27)$$

$$\mathbf{i}_s^{dq} = C_s \frac{d}{dt} \mathbf{v}_{Cs}^{abc} - G \mathbf{m}_r^{dq} i_{dc} \quad (28)$$

$$G \left[\mathbf{m}_r^{dq} \right]^T \mathbf{v}_{Cr}^{dq} = L_{dc} \frac{d}{dt} i_{dc} + i_{dc} m_i \sin(\omega_i t + \alpha_i) \quad (29)$$

where

$$\mathbf{W} = \begin{bmatrix} 0 & -\omega_s \\ \omega_s & 0 \end{bmatrix} \quad (30)$$

Thus, it is possible to define the non-linear control in order to regulate the dq components of the cell input current in a decoupled way. The DC current and the displacement power factor are regulated using the previous controller and their references are set in a master loop.

A. Input cell current control loop

The input current controller is defined by a PI controller that relates an auxiliary variable \mathbf{u}_p^{dq} and the modulating signal such that

$$\mathbf{m}_r^{dq} = \frac{1}{A_s} \left[D_s \mathbf{u}_p^{dq} + \mathbf{F}_s \begin{bmatrix} \mathbf{i}_s^{dq} \\ \frac{d}{dt} \mathbf{i}_s^{dq} \end{bmatrix} - \mathbf{B}_s \begin{bmatrix} \mathbf{x}_s \\ \mathbf{p}_s \\ \frac{d}{dt} \mathbf{p}_s \end{bmatrix} \right] \quad (31)$$

where

$$\mathbf{x}_s = \left[i_s^d \quad i_s^q \quad v_{Cs}^d \quad v_{Cs}^q \quad i_{dc} \right]^T, \quad (32)$$

$$\mathbf{p}_s = \left[v_s^d \quad v_s^q \right]^T, \quad (33)$$

$$A_s = G_r i_{dc} / (C_s L_s), \quad (34)$$

$$\mathbf{B}_s = \begin{bmatrix} -\omega_r^2 - 1 / (L_s C_s) & 0 \\ 0 & -\omega_r^2 - 1 / (L_s C_s) \\ 0 & 2\omega_s / L_s \\ -2\omega_s / L_s & 0 \\ 0 & 0 \\ 0 & -2\omega_s / L_s \\ 2\omega_s / L_s & 0 \\ 1 / L_s & 0 \\ 0 & 1 / L_s \end{bmatrix}. \quad (35)$$

$$D_s = k_2 \quad (36)$$

$$\mathbf{F}_s = \begin{bmatrix} -k_2 & 0 & -k_1 & 0 \\ 0 & -k_2 & 0 & -k_1 \end{bmatrix} \quad (37)$$

In order to compensate small parameters differences when (31) is computed, an integrator is used to relate \mathbf{u}_p^{dq} and the cell input current references $\mathbf{i}_{s,ref}^{dq}$ as is shown in (38). Hence, a third order transfer function between $\mathbf{i}_{s,ref}^{dq}$ and \mathbf{i}_s^{dq} is obtained and its dynamic is given by k_1 , k_2 and $T_{i, is}$, (39). Imposing a desired settling time, these parameters are calculated with the ITAE criterion as shown in (40)-(42).

$$\frac{\mathbf{u}_s^d}{i_{s,ref}^d} = \frac{\mathbf{u}_s^q}{i_{s,ref}^q} = \frac{1}{T_{i, is} s}, \quad (38)$$

$$\frac{i_s^d}{i_{s,ref}^d} = \frac{i_s^q}{i_{s,ref}^q} = \frac{k_2}{T_{i, is} s^3 + k_1 s^2 + k_2 s + k_2 / T_{i, is}} \quad (39)$$

$$k_1 = 13.195 / t_{s, ip}, \quad (40)$$

$$k_2 = 122.231 / t_{s, ip}^2, \quad (41)$$

$$T_{i, ip} = 0.285 t_{s, ip} \quad (42)$$

B. DC current control loop

A master controller over the i_s^d control loop is used in order to regulate the DC current. Performing the power balance in the rectifier, it is possible to write that

$$v_{Cs}^d i_s^d + v_{Cs}^q i_s^q = -L_{dc} i_{dc} \frac{d}{dt} i_{dc} - i_{dc}^2 R_{dc} - \overline{p_o} \quad (43)$$

where $\overline{p_o}$ is the continuous component of the inverter power as show in (8). This is a convenient way because magnetic couplings compensate the oscillating power. Defining the auxiliary input u_{idc} to control i_{dc} as

$$u_{idc} = L_{dc} \frac{d}{dt} i_{dc} \quad (44)$$

it is possible to write the reference for the d component of the cell input current, $i_{s,ref}^d$, using (43) and (44) such that

$$i_{s,ref}^d = \frac{1}{v_{Cs}^d} \left[u_{idc} i_{dc} - i_{dc}^2 R_{dc} - \overline{p_o} - v_{Cs}^q i_s^q \right] \quad (45)$$

The auxiliary input defined in (44) requires the computation of (45) and small parameter variations will lead to steady state error. Therefore, a PI regulator between the auxiliary input u_{idc} and the DC current reference $i_{dc,ref}$, given by

$$\frac{u_{idc}}{i_{dc,ref}} = k_{p,i_{dc}} + \frac{k_{i,i_{dc}}}{s} \quad (46)$$

is added, leading to a second order transfer function between $i_{dc,ref}$ and i_{dc} as

$$\frac{i_{dc}}{i_{dc,ref}} = \frac{k_{i,i_{dc}} + k_{p,i_{dc}} s}{L_{dc} s^2 + k_{p,i_{dc}} s + k_{i,i_{dc}}} \quad (47)$$

A first order filter between $i_{dc,ref}$ and $i_{dc,ref}$ is added to compensate the zero in (47) (Fig. 3). Finally, the previous block allows a standard second order relation between $i_{dc,ref}$ and i_{dc} . Thus, it is possible to define the PI parameters as a function of the desired natural frequency $\omega_{o,i_{dc}}$ and damping ratio $\zeta_{i_{dc}}$ for this loop as

$$k_{i,i_{dc}} = \omega_{o,i_{dc}}^2 L_{dc} \quad (48)$$

and

$$k_{p,i_{dc}} = 2\zeta_{i_{dc}} \sqrt{L_{dc} k_{i,i_{dc}}} \quad (49)$$

Because the DC link current i_{dc} loop is the master loop, it is recommendable to set its settling time at least 5 times slower than $t_{s,ip}$.

C. Displacement Power Factor Control

This loop basically sets the reference for the inner $i_{s,ref}^q$ loop for a given power factor reference $pf_{pcc,ref}$. This reference can be set by an external loop if it is desired to compensate the reactive power with the MC-CSC or can be set to $i_{s,ref}^q = 0$ in order to have unitary displacement power factor in each cell. The present work considers the latter case.

D. Master Output Voltage Control

The proposed scheme controls the inner state variables of each cell in a decoupled way. Over this control a master controller can be defined in order to set a desired voltage and frequency at the load side. In this case, the DC current reference is adjusted instead.

IV. CASE OF EXAMPLE

A 110 kVA load fed by six cells was simulated in the PSim software with the parameters given in Table I. Each cell is supplied by a 550 V_{rms} and ideal transformers are considered to couple the DC sides of three cells in order to provide oscillating power compensation. The DC reactor has been designed in order to have 55% of 2nd DC current harmonic for a 10 Hz output frequency ($\omega_i = 61.4$ rad/s) without using magnetic couplings among DC link.

Table I - Simulation Parameters

Parameter	Value
Load	R_l 40 Ω
	L_l 80 mH
Input Filter	L_s 12 mH
	C_s 55 μ F
DC Inductor (without magnetically coupling)	L_{dc}^* 400 mH
DC Inductor (used in simulation)	L_{dc} 30 mH
Output Capacitor	C_o 10 μ F
Rectifier Modulating Frequency	1050 Hz
Inverter Modulating Frequency	1000 Hz
Settling Time Input Current Controller	7 ms
DC Current Control	$\omega_{o,i_{dc}}$ 125.3 rad/s
	$\zeta_{i_{dc}}$ 1

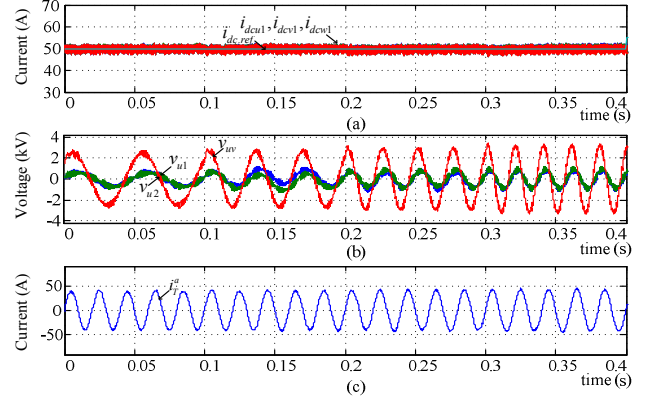


Fig. 4 Performance under inverter frequency changes; (a) DC Current, (b) output voltage and load voltage, (c) transformer input current.

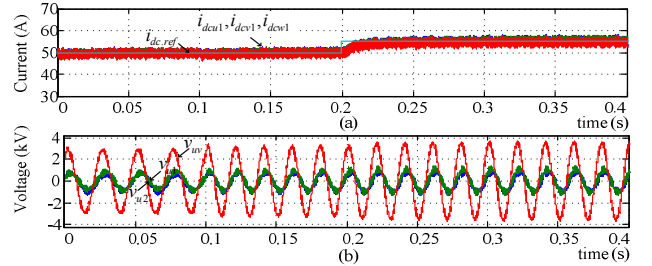


Fig. 5 DC controller performance for 10% reference step change; (a) DC Current (b) output voltage and load voltage.

A. Oscillating Power Compensation under Frequency Changes

Fig. 4 shows the proposed topology and control scheme performance with an oscillating power compensation by means of magnetic couplings with step changes of 10 Hz every 100 ms – from 20 Hz in $t = 0$ ms up to 50 Hz in $t = 500$ ms – in the output frequency (Fig. 4b). Thanks to the capacitive filter in each inverter, the load voltage has low distortion. Additionally, magnetic couplings are able to compensate the oscillating power while the DC control loop keeps the DC current in the desired level (50 A) with a current ripple that is function of the DC inductor in each cell. According to (12), to obtain a similar quality for the DC current, a 400 mH DC inductor is required, but using the magnetic coupling, just a 30 mH DC inductor can be used. Because the oscillating power is compensated with the

magnetic couplings, the rectifier must inject the continuous power component in order to have a transformer input current with low distortion (Fig. 4c).

B. DC Current Control Performance

In order to evaluate the DC control loop behavior, a step change of 10 % is applied at $t = 200$ ms (Fig. 5a). After this change, the load voltage increases its value in 10%. On the other hand, the output voltage quality (Fig 5b) is maintained.

V. EXPERIMENTAL TEST

A three-cells low-power prototype was implemented. Fig. 6 shows the performance in open loop for 50 Hz output frequency and a 3.5 A DC current. Because the rectifiers are modulated in open loop using constant \mathbf{m}_r^{dq} , all the oscillating power is compensated by the magnetic coupling as can be observed in the transformer coupling voltage. Similarly, neither 3rd output voltage harmonic nor 2nd current harmonic are present.

VI. CONCLUSIONS

This work shows the problems due to the oscillating power drained by single-phase inverters in a Multi-Cell Current Source Topology. To avoid oversizing the DC reactor due to the oscillating power, magnetic coupling among three DC links that feed different load phases is used. The topology can achieve a high quality overall supply current – because of the harmonic cancellation effect of the multipulse transformer – and a high load voltage quality due to the use of capacitive filter at the cell output. The proposed nonlinear control scheme allows each power cell to be controlled in a decoupled way. The DC reactor size is reduced significantly without an important 2nd harmonic in the DC current. Simulated results shows the feasibility of the proposed topology and control, which are corroborated with preliminary experimental results. For the studied case, a reduction from 400 mH to 30 mH is achieved thanks to the use of magnetic couplings.

ACKNOWLEDGMENT

The authors wish to thank the financial support from the Chilean Fund for Scientific and Technological Development CONICYT / FONDECYT / 1110794, CONICYT / FONDECYT / 15110019 and the technical support provided by the Applied Digital Control Laboratory, University of Concepcion, Chile.

REFERENCES

- [1] J. Rodriguez, S. Bernet, B. Wu, J. Pontt, S. Kouro, "Multilevel Voltage-Source Converter Topologies for Industrial Medium-Voltage Drives," *IEEE Trans. On Indus. Electron.* Vol 54, No. 6, pp. 2930-2945, December 2007.
- [2] Malinowski, M.; Gopakumar, K.; Rodriguez, J.; Pérez, M.A., "A Survey on Cascaded Multilevel Inverters," in *IEEE Trans. on Indus. Electron.*, vol.57, no.7, pp.2197,2206, July 2010
- [3] B. Wu, J. Pontt, J. Rodriguez, S. Bernet, S. Kouro, "Current-Source Converter and Cycloconverter Topologies for Industrial Medium-Voltage Drives," *IEEE Trans. on Indus. Electron.*, Vol. 55, No. 7, pp. 2786-2797 July 2008
- [4] Bin Wu; Dewan, S.B.; Slemon, G.R., "PWM-CSI inverter for inductionmotor drives," in *IEEE. Trans. on Indus. Applicat.*, vol.28, no.1, pp.64,71, Jan/Feb 1992
- [5] E. Wiechmann, P. Aqueveque, R. Burgos, J. Rodriguez "On the efficiency of voltage source and current source inverters for high-power

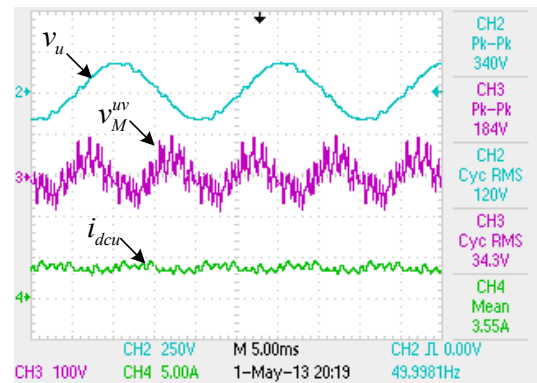


Fig. 6 Key waveform for oscillating power compensation

- drives," *IEEE Trans. on Indus. Electron.*, Vol. 55, No. 4, pp. 1771-1782, April 2008
- [6] Zargari, N.R., Joos, G., Ziogas, P.D. "Input filter design for PWM current-source rectifiers," *IEEE Trans. on Ind. Apps.*, vol. 30, n° 6, pp 1573-1579, Nov./Dec. 1994.
- [7] P. Melin, J. Espinoza, N Zargari, M. Sánchez & J Guzman "Modeling issues in three-phase current source rectifiers that use damping resistors," *Conf. Rec. ISIE'06*, Vol. 2, pp 1247 - 1252, July 2006..
- [8] J. Espinoza, G. Joos, L Morán "Decoupled control of the active and reactive power in three-phase PWM rectifier based on non-linear control strategies," *Conf. Rec. PESC'1999*, Vol.1, pp 131-136, June/July 1999.
- [9] Espinoza, J.R.; Moran, L.A.; Guzman, J.I., "Multi-Level Three-Phase Current Source Inverter based AC Drive for High Performance Applications," in *Conf. Rec. PESC 2005*. pp.2553,2559, 16-16 June 2005
- [10] Guzman, J.I.; Espinoza, J.R.; Zargari, N.R.; Moran, L.A., "Selective Harmonic Elimination in Multi-Modules Three-Phase Current-Source Converters," in *Conf. Rec. ISIE 2006*, pp.1241,1246, 9-13 July 2006
- [11] Espinoza, J.R.; Moran, L.A.; Zargari, N.R., "Multi-Level Three-Phase Current Source Inverter based Series Voltage Compensator," in *Conf. Rec. PESC 2005*, pp.2264,2269, 16-16 June 2005
- [12] Melin, P.E.; Espinoza, J.R.; Munoz, J.A.; Baier, C.R.; Espinosa, E.E., "Concepts of decoupled control for a shunt active filter based on multilevel current source converters," in *Conf. Rec. ISIE 2010*, pp.742,747, 4-7 July 2010
- [13] Aguirre, M.P.; Calvino, L.; Valla, M.I., "Multilevel Current-Source Inverter With FPGA Control," in *IEEE Trans. on Indus. Electron.*, vol.60, no.1, pp.3,10, Jan. 2013
- [14] Suroso, S.; Noguchi, T., "Multilevel Current Waveform Generation Using Inductor Cells and H-Bridge Current-Source Inverter," in *Trans. on Power Electron.*, vol.27, no.3, pp.1090,1098, March 2012
- [15] Vazquez, N.; Lopez, H.; Hernandez, C.; Vazquez, E.; Osorio, R.; Arau, J., "A Different Multilevel Current-Source Inverter," in *IEEE Trans. on Indust. Electron.*, no.8, pp.2623,2632, Aug. 2010
- [16] Melin, P.E.; Espinoza, J.R.; Zargari, N.R.; Moran, L.A.; Guzman, J.I., "A novel multi-level converter based on current source power cell," in *Conf. Rec. PESC 2008*. pp.2084,2089, 15-19 June 2008
- [17] Melin, P.E.; Espinoza, J.R.; Baier, C.R.; Rohten, J.A.; Ramirez, R.O.; Moran, L.A., "Improved control scheme towards reduced DC link inductors in a Multi-Cell Topology based on Current Source Converters," in *conf. rec IECON 2012* pp.488,493, 25-28 Oct. 2012.
- [18] Baier, C.R.; Espinoza, J.R.; Melin, P.E.; Espinoza, E.; Munoz, J., "A novel multi-level CSI based topology with inter-cell magnetic couplings for minimum DC storage components," in *conf. rec ISIE 2010*, vol., no., pp.3193,3198, 4-7 July 2010.
- [19] Baier, C.R.; Melin, P.E.; Espinoza, J.R.; Munoz, J.; Guzman, J.I., "A novel multi-level topology based on current source power cells for high performance applications," in *Conf. Rec ICIT 2010*, pp.1333,1338, 14-17 March 2010
- [20] Perez, M.A.; Lizana, R.; Azocar, C.; Rodriguez, J.; Bin Wu "Modular multilevel cascaded converter based on current source H-bridges cells", in *Conf. Rec. IECON 2012*, pp. 3443 - 3448, October 2012.